On the Robustness of Oversampled Filter Bank Multi Carrier Systems against Frequency Offset

Siavash Rahimi
McGill University
Department of Electrical and Computer Engineering
3480 University Street, Montreal, Quebec H3A0E9
siavash.rahimi@mail.mcgill.ca

Benoit Champagne
McGill University
Department of Electrical and Computer Engineering
3480 University Street, Montreal, Quebec H3A0E9
benoit.champagne@mcgill.ca

***Abstract*—In this paper, we study the effect of oversampling in a perfect reconstruction (PR) filter bank multi carrier (FBMC) system recently proposed by the authors. Particularly, we investigate the performance of this system in the presence of carrier frequency offset (CFO). We show that the CFO introduces interference components in the receiver. By exploiting the statistical properties of the received subband signals, the average of the signal-to-interference ratio (SIR) is derived to exhibit the tradeoff between performance and efficiency. Furthermore, bit-error-rate (BER) comparisons of FBMC systems with different oversampling ratios over frequency-selective and additive white Gaussian noise (AWGN) channels in the presence of CFO are presented. These results confirm that oversampling increases robustness of the system against CFO.**

I. Introduction

Multicarrier modulation (MCM) is currently the method of choice for high speed wireless communications, particularly over frequency-selective channels. Its sensitivity to imperfect synchronization, including carrier frequency offset (CFO), however, limits its performance and requires employing some countermeasure techniques [1]–[3]. The most common realization of MCM in standards has been orthogonal frequency division multiplexing (OFDM). By employing cyclic prefix (CP) and sacrificing spectral efficiency, OFDM can prevent inter-symbol interference (ISI). However, there are two harmful effects on OFDM caused by CFO: the reduction of signal amplitude of each subcarrier and the introduction of inter-carrier interference (ICI) due to the loss of orthogonality between subcarriers [1], [2].

To avoid such drawbacks, filter bank multi carrier (FBMC) systems have been proposed which benefit from improved frequency selectivity through the use of longer, and thus better shaped prototype filters in the frequency domain. FBMC systems consist of a synthesis (transmit) and analysis (receive) filter banks (FB), interconnected by a transmission channel [4]–[7]. The synthesis bank combines its M subband input signals sampled at the low rate F_s, into a single output signal with higher sampling rate KF_s for transmission over the channel, where K denotes the upsampling factor. The analysis bank decomposes the baseband channel output with sampling rate KF_s, into its M constituent subband components with rate F_s.

The FB is said to be critically sampled if $K = M$, and oversampled if $K > M$, while perfect reconstruction (PR) refers to a condition where the output of the tandem combination of the transmit and receive FBs (i.e., ideal channel) is a delayed version of the input. Compared to the critically sampled FBs, oversampled FBs benefit from additional design freedom that can be used to obtain the PR property *and* additional spectral containment, hence better noise immunity within each subband [5]–[7]. These improvements come at the cost of increased redundancy, and loss of spectral efficiency. Therefore, these redundancies in oversampled FBs should not exceed those introduced by the cyclic prefix (CP) in OFDM systems to remain competitive with them.

This work was supported by InterDigital Canada, the Natural Sciences and Engineering Research Council of Canada, and the Government of Quebec under the PROMPT program.

FBMC systems, like OFDM, are sensitive to CFO; however, it has been shown that oversampled PR FBMCs can outperform OFDM systems in the presence of CFO or other channel impairments [6], [8]–[10]. Therefore, the tradeoff between interference and spectral efficiency of oversampled FBMC system is a major factor for the system design and comparison with OFDM. In order to exhibit this tradeoff, in [11], the interference caused by the channel frequency selectivity is quantified. However, synchronization error including CFO is not considered in the analysis. In [8], the authors briefly discuss the frequency misalignment effect on the performance of FBMC system and focus on the techniques of offset correction. Recently, the effects of CFO on general FBMC systems based on studies and simulation of practical systems has been presented in [12]. Moreover, in the special case of critically sampled nearly-PR FBMC system, these effects are reported in [9].

In this paper, to demonstrate and quantize the advantages of oversampled PR FBMC system in combating transmission impairments such as CFO, closed form expressions of signal-to-interference ratio (SIR) of the system proposed in [6] are provided. The CFO is modelled by means of a rotating phase $\varphi(m) = e^{j(2\pi\mu m)}$ multiplying the baseband signal, where μ indicates the frequency offset normalized with respect to subband spacing. Furthermore, the average bit-error-rate (BER) in the presence of CFO for OFDM and FBMC systems with different oversampling ratios in AWGN and frequency-selective channels is presented. Benefiting from PR property and oversampling guard bands, it is evident that the considered system outperforms OFDM and their CFO induced interference reduces by larger oversampling ratios. Using these measures, the tradeoff between spectral efficiency and system performance is illuminated to facilitate the design process.

The paper is organized as follows. In Section II, we discuss the system model of oversampled PR FBMC system. In Section III, the demodulated signal is analyzed in the presence of CFO. Closed form expression of SIR is derived in Section IV. Section V is devoted to the presentation of experimental results. Finally, Section VI concludes the work.

II. Oversampled PR FBMC System Model

The FBMC system under consideration is depicted in Fig. 1, where $x_i[n]$ denotes the complex-valued data sequence transmitted on the ith subband, $i \in \{0, \ldots, M-1\}$, at discrete-time nT, where $T = F_s^{-1}$ and $n \in \mathbb{Z}$ is the discrete-time index at the low sampling rate F_s. In DFT modulated FBMCs, the transmit and the receive subband filters can be derived from common prototype filters of length D, with

978-1-4673-0762-8/12/$31.00 ©2012 IEEE

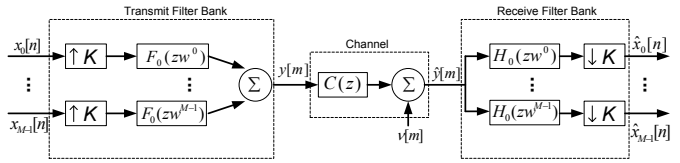

Fig. 1. DFT modulated oversampled filter bank transceiver

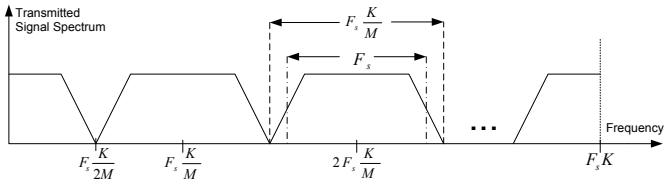

Fig. 2. Frequency spectrum of an oversampled FBMC system

respective system functions $F_0(z) = \sum_{n=0}^{D-1} f_0(n)z^{-n}$ and $H_0(z) = \sum_{n=0}^{D-1} h_0(n)z^{n}$[1]. Defining $w = e^{-j2\pi/M}$, the transmit and receive filter for the ith subband ($i \in \{1, \ldots, M-1\}$) are respectively obtained as

$$F_i(z) = F_0(zw^i) \quad , H_i(z) = H_0(zw^i). \tag{1}$$

In this work, D is restricted to be a multiple of M and K, where the parameters M and K represent the number of subbands and the upsampling/downsampling factor, respectively. We also use P to denote the least common multiple of M and K, and therefore: $D = d_P P$, with integer d_P. As stated before, we consider oversampled PR FBMC [6], where $K > M$. In this case, as shown in Fig. 1, the baseband discrete-time signal is given by

$$y(m) = \sum_{q=-\infty}^{\infty} \sum_{i=0}^{M-1} x_i(q) f_i(m - qK). \tag{2}$$

The transmission channel is modelled as an FIR filter with system function $C(z) = \sum_{l=0}^{Q-1} c[l]z^{-l}$; the channel output is corrupted by the additive noise $\nu[m]$. The input-output relation of the channel can be expressed as

$$\hat{y}(m) = \sum_{l=0}^{Q-1} c(l)y(m-l) + \nu(m). \tag{3}$$

At the receiver side, the received signal is filtered with a bank of matched filters and downsampled to the factor K, thus for each subband, the constructed signal $\hat{x}_i(n)$ can be written as

$$\hat{x}_i(n) = \sum_{q=-\infty}^{\infty} \hat{y}(q) h_i(q - nK). \tag{4}$$

A. Perfect Reconstruction

To ensure that transmission is free from ISI and ICI, the prototype filter characteristics are often chosen to satisfy a PR constraint [5]. As in [6], to achieve PR property, it is assumed that the transmit and receive prototype filters are paraconjugate of each other, i.e. $H_0(z) = \tilde{F}_0(z)$ or equivalently, $h_0(n) = f_0^*(n)$. Therefore, the PR conditions (i.e., $\hat{x}_i(n) = x_i(n)$ for all $i \in \{0, \ldots, M-1\}$ and $n \in \mathbb{Z}$) in the case of an ideal channel (i.e. $C(z) = 1$ and $\nu(m) = 0$) are expressed in the time domain as [4]

$$\sum_{q=-\infty}^{\infty} f_i(q - pK) f_j^*(q - nK) = \delta_{i-j}\delta_{n-p}, \tag{5}$$

for all $i, j \in \{0, \ldots, M-1\}$ and $n, p \in \mathbb{Z}$, where δ_k is the Kronecker delta ($\delta_0 = 1$ and $\delta_k = 0$ if $k \neq 0$).

B. Oversampling and Spectral Efficiency

Fig. 2 illustrates the spectral characteristics of the transmitted signal [5]. F_sK/M is the frequency spacing between adjacent subbands, where the rate of input signal in each band is $F_s = 1/T$. In other words, the transmission bandwidth $B = KF_s$ is divided to M equally spaced subchannels, where each input channel has a bandwidth of F_s and totally they have a bandwidth of MF_s. Therefore, the spectral efficiency η of the system can be derived as

$$\eta = \frac{MF_s}{KF_s} = M/K \tag{6}$$

It is evident that larger oversampling ratio increases the frequency spacing and decreases the spectral efficiency. Similarly, OFDM system with M subbands employs CP of length L in order to combat the channel impairment and to remove ISI. The spectral efficiency in this case is $\eta = M/(M+L)$.

III. Effect of Carrier Frequency Offset

Let us consider that the signal $y(m)$ is transmitted through an AWGN channel as shown in the baseband equivalent in Fig. 1. The received signal $\hat{y}(m)$ in the presence of an additive white Gaussian noise $\nu(m)$ with zero mean and variance $E[|\nu(m)|^2] = N_0/E_s$, is given by

$$\hat{y}(m) = e^{j2\pi\mu m} y(m) + \nu(m), \tag{7}$$

where μ is a normalized CFO with respect to subband spacing F_sK/M. By employing the paraconjugate of transmit filters on the receiver side, the constructed signal $\hat{x}_i(n)$ for each subband can be rewritten as

$$\hat{x}_i(n) = \sum_{q=-\infty}^{\infty} \hat{y}(q) f_i^*(q - nK). \tag{8}$$

Furthermore, $\hat{x}_i(n)$ can be rewritten in terms of input signals $x_i(n)$ as

$$\begin{aligned}
\hat{x}_i(n) \quad = \quad & \sum_{q=-\infty}^{\infty} e^{j2\pi\mu q} x_i(n) f_i(q - nK) f_i^*(q - nK) \\
& + \sum_{\substack{p,q=-\infty \\ p\neq n}}^{\infty} e^{j2\pi\mu q} x_i(p) f_i(q - pK) f_i^*(q - nK) \\
& + \sum_{p,q=-\infty}^{\infty} \sum_{\substack{r=0 \\ r\neq i}}^{M-1} e^{j2\pi\mu q} x_r(p) f_r(q - pK) f_i^*(q - nK) \\
& + \sum_{q=-\infty}^{\infty} \nu(q) f_i^*(q - nK),
\end{aligned} \tag{9}$$

where first, second, third and fourth terms correspond to the attenuated signal, ISI terms, ICI terms, and channel additive noise, respectively. By defining $\Gamma_{i,r}^{\mu}(p, n)$ as

$$\Gamma_{i,r}^{\mu}(p, n) = \sum_{q=-\infty}^{\infty} e^{j2\pi\mu q} f_r(q - pK) f_i^*(q - nK) \tag{10}$$

[1]For convenience in analysis, $H_i(z)$ is assumed non-causal; in practice, causality can be restored simply by introducing an appropriate delay in the receiver.

and substituting it in (9), we can write

$$\hat{x}_i(n) = x_i(n)\Gamma^{\mu}_{i,i}(n,n) + \sum_{\substack{p=-\infty \\ p\neq n}}^{\infty} x_i(p)\Gamma^{\mu}_{i,i}(p,n) + \sum_{p=-\infty}^{\infty}\sum_{\substack{r=0 \\ r\neq i}}^{M-1} x_r(p)\Gamma^{\mu}_{i,r}(p,n) + \nu_i(n), \quad (11)$$

where $\nu_i(n) = \sum_{q=-\infty}^{\infty} \nu(q) f_i^*(q-nK)$. By assuming normalized input signal, i.e. $E[|x_i|^2] = 1$, and the fact that the background noise is independent of the ICI and ISI terms, the signal to interference plus noise ratio (SINR) of the ith subcarrier at time instant n can be expressed:

$$\rho_{\text{SINR}}(i,n) = \frac{|\Gamma^{\mu}_{i,i}(n,n)|^2}{\sum_{r=0}^{M-1}\sum_{p=-\infty}^{\infty}|\Gamma^{\mu}_{i,r}(p,n)|^2 - |\Gamma^{\mu}_{i,i}(n,n)|^2 + N_0/E_s} \quad (12)$$

If we employ the quadrature phase-shift keying (QPSK) constellation, then the lower bound for the average BER of the system over the AWGN channel with CFO is given by

$$P_b = Q\left(\sqrt{2\rho_{\text{SINR}}(i,n)}\right)\left(1 - \frac{1}{2}Q\left(\sqrt{2\rho_{\text{SINR}}(i,n)}\right)\right) \quad (13)$$

IV. SIR Analysis

To have a better understanding of CFO induced interferences, we derive the SIR to analyze the tradeoff between the spectral efficiency and performance degradation of the transceiver over the AWGN channel with CFO. The average energy of the signal S can be written as

$$S = \frac{1}{M}\sum_{i=0}^{M-1}|\Gamma^{\mu}_{i,i}(n,n)|^2 \quad (14)$$

Furthermore, the interference level I which is the average of all the subbands interferences is

$$I = \frac{1}{M}\sum_{i=0}^{M-1}\left(\sum_{r=0}^{M-1}\sum_{p=-\infty}^{\infty}|\Gamma^{\mu}_{i,r}(p,n)|^2 - |\Gamma^{\mu}_{i,i}(n,n)|^2\right) = \frac{1}{M}\sum_{i=0}^{M-1}\sum_{r=0}^{M-1}\sum_{p=-\infty}^{\infty}|\Gamma^{\mu}_{i,r}(p,n)|^2 - S \quad (15)$$

Therefore, the SIR denoted by $\rho = S/I$ is given by

$$\rho = \frac{\frac{1}{M}\sum_{i=0}^{M-1}|\Gamma^{\mu}_{i,i}(n,n)|^2}{\frac{1}{M}\sum_{i=0}^{M-1}\left(\sum_{r=0}^{M-1}\sum_{p=-\infty}^{\infty}|\Gamma^{\mu}_{i,r}(p,n)|^2 - |\Gamma^{\mu}_{i,i}(n,n)|^2\right)} \quad (16)$$

In order to simplify the SIR , $|\Gamma^{\mu}_{i,r}(p,n)|^2$ is developed by using the fact that subband filters are DFT modulated, i.e. $f_i(p) = f_0(p)e^{-j2\pi ip/M}$.

$$|\Gamma^{\mu}_{i,r}(p,n)|^2 = \sum_{q,q'=-\infty}^{\infty} e^{j2\pi\mu(q-q')} f_r(q-pK) f_i^*(q-nK) \times f_r^*(q'-pK) f_i(q'-nK) = \sum_{q,q'=-\infty}^{\infty} e^{j2\pi(\mu-\frac{i-r}{M})(q-q')} f_0(q) f_0^*(q+(p-n)K) \times f_0^*(q') f_0(q'+(p-n)K). \quad (17)$$

Furthermore, by considering $v = i - r$ and $l = p - n$, (17) can be rewritten as

$$|\Gamma^{\mu}_{i,r}(p,n)|^2 = |\gamma^{\mu}_{v}(l)|^2 \quad (18)$$

where $\gamma^{\mu}_{v}(l)$ is

$$\gamma^{\mu}_{v}(l) = \sum_{q=-\infty}^{\infty} e^{j2\pi q(\mu-\frac{v}{M})} f_0(q) f_0^*(q+lK) \quad (19)$$

It is clear that due to the DFT modulation, the signal and interference level are same for all the subbands. The time average signal power S can be obtained as the following form:

$$S = \frac{1}{M}\sum_{i=0}^{M-1}|\Gamma^{\mu}_{i,i}(n,n)|^2 = |\gamma^{\mu}_{0}(0)|^2 = \sum_{q=-\infty}^{\infty}\sum_{q'=-\infty}^{\infty} e^{j2\pi\mu(q-q')}|f_0(q)|^2|f_0(q')|^2. \quad (20)$$

Similarly, I can be rewritten as

$$I = \frac{1}{M}\sum_{i=0}^{M-1}\sum_{r=0}^{M-1}\sum_{p=-\infty}^{\infty}|\Gamma^{\mu}_{i,r}(p,n)|^2 - S = \sum_{v=0}^{M-1}\sum_{l=-\infty}^{\infty}|\gamma^{\mu}_{v}(l)|^2 - |\gamma^{\mu}_{0}(0)|^2 \quad (21)$$

Finally, by inserting (20) and (21) into (16), closed form expression of SIR in terms of prototype filter coefficients can be derived

$$\rho = \frac{|\gamma^{\mu}_{0}(0)|^2}{\sum_{v=0}^{M-1}\sum_{l=-\infty}^{\infty}|\gamma^{\mu}_{v}(l)|^2 - |\gamma^{\mu}_{0}(0)|^2} \quad (22)$$

A. SIR for Small CFOs

It is straightforward to derive the limit of $\Gamma^{\mu}_{i,r}(p,n)$ when μ approaches zero by using PR equation (5) as

$$\lim_{\mu\to 0}\Gamma^{\mu}_{i,r}(p,n) = \sum_{q=-\infty}^{\infty}\lim_{\mu\to 0} e^{j2\pi\mu q} f_r(q-pK) f_i^*(q-nK) = \sum_{q=-\infty}^{\infty} f_r(q-pK) f_i^*(q-nK) = \delta_{i-r}\delta_{n-p} \quad (23)$$

Therefore, $\lim S$ when $\mu \to 0$ can be derived as

$$\lim_{\mu\to 0} S = \lim_{\mu\to 0}|\Gamma^{\mu}_{i,i}(n,n)|^2 = |\delta_{i-i}\delta_{n-n}|^2 = 1 \quad (24)$$

Moreover, it can be stated about equation (15)

$$\lim_{\mu\to 0} I = \lim_{\mu\to 0}\frac{1}{M}\sum_{i=0}^{M-1}\sum_{r=0}^{M-1}\sum_{p=-\infty}^{\infty}|\Gamma^{\mu}_{i,r}(p,n)|^2 - S \quad (25)$$

$$\lim_{\mu\to 0} I = \lim_{\mu\to 0}\frac{1}{M}\sum_{i=0}^{M-1}\sum_{r=0}^{M-1}\sum_{p=-\infty}^{\infty}|\delta_{i-r}\delta_{n-p}|^2 - 1 = 0 \quad (26)$$

We can observe that I approaches zero as μ approaches zero, which is caused by the PR property of the system. Thus, $\rho = S/I$ will go to infinity around $\mu = 0$ where the ISI and ICI terms are negligible due the PR constraint of the system.

Finally, we investigate (22), and try to approximate SIR for small CFOs. Since q just varies in the range of filter length D in (18), when μ is in the vicinity of zero, (18) can be well approximated by keeping the first two dominant terms of Taylor series $e^{j2\pi\mu(q-q')} \simeq$

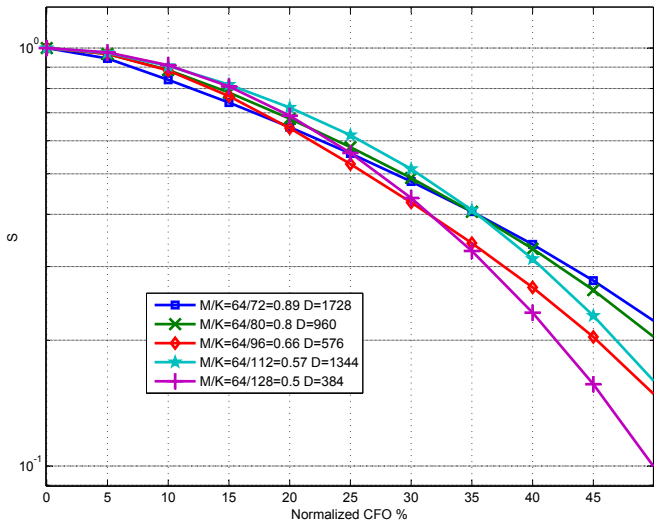

Fig. 3. Signal power $S = |\gamma_0^{\mu}(0)|^2$

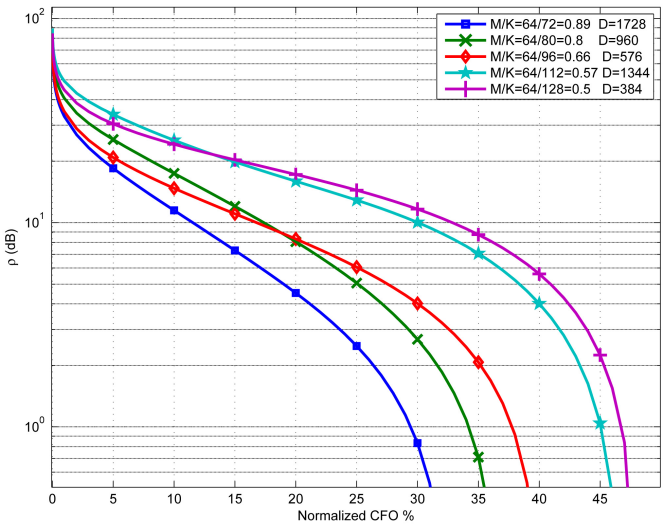

Fig. 4. signal-to-interference ratio ρ (dB)

$1+j2\pi\mu(q-q')$. Consequently, by using PR property (5), we obtain

$$\begin{aligned} |\gamma_v^{\mu}(l)|^2 &\simeq |\sum_{q=-\infty}^{\infty} e^{-j2\pi\frac{v}{M}q} f_0(q) f_0^*(q+lK)|^2 + j2\pi\mu C_v(l) \\ &= |\sum_{q=-\infty}^{\infty} f_v(q) f_0^*(q+lK)|^2 + j2\pi\mu G_v(l) \\ &= \delta_v\delta_l + j2\pi\mu G_v(l) \end{aligned} \quad (27)$$

where $G_v(l)$ is defined as

$$\begin{aligned} G_v(l) &= \sum_{q,q'=-\infty}^{\infty} (q-q') e^{-j2\pi\frac{v}{M}(q-q')} \\ &\quad \times f_0(q) f_0^*(q+lK) f_0^*(q') f_0(q'+lK) \end{aligned} \quad (28)$$

Consequently, (22) can be approximated as

$$\rho \simeq \frac{1+j2\pi\mu G_0(0)}{j2\pi\mu \sum_{v=0}^{M-1}\sum_{l=-\infty}^{\infty} G_v(l) - G_0(0)} \quad (29)$$

It can be shown that $G_0(0) = 0$; therefore, we can further simplify the SIR as

$$\rho \simeq \frac{1}{\mu}\left(\frac{1}{j2\pi \sum_{v=0}^{M-1}\sum_{l=-\infty}^{\infty} G_v(l)}\right) \quad (30)$$

It can be observed in (30) that when μ is small, SIR is proportional with $1/\mu$.

V. Experimental Results

This section is dedicated to the performance comparison of oversampled PR FBMC systems in the presence of CFO, where these systems have $M = 64$ subcarriers with several different upsampling factors $K = 72, 80, 96, 112, 128$. Therefore, spectral efficiency $\eta = M/K$, defined in Section II-B as the ratio of the number of subbands over the upsampling factor, varies from $\eta = 0.5$ to $\eta = 0.89$. According to the design procedure [6], prototype filter length $D = d_P P$, where P is the least common multiple of M and K and integer d_P. Concerning implementation complexity, we fixed $d_P = 3$ for all the oversampled FBMCs which denotes the number of non-zero filter taps in the polyphase structure of the system. Thus, the filter lengths are $D = 1728, 960, 576, 1344, 384$ corresponding to upsampling factor $K = 72, 80, 96, 112, 128$, respectively.

A. Oversampling Effect on Signal and Interference

In Fig. 3, the attenuated signal power values S of the mentioned FBMC systems for different CFOs are depicted. It has been observed that the values of S for μ and $-\mu$ are equal and it is a even function with respect to CFO. Therefore, in this experiment, μ is just varied between 0 to 50% of carrier spacing (subband spacing is $F_s K/M$). As expected, the highest value of S is at $\mu = 0$ which coincides with PR case. In accordance with analysis in Section IV-A, Fig. 3 indicates that the signal attenuation in the presence of small CFOs, is similar among the different FBMCs. However, with larger frequency offsets, the FBMC systems with longer filters benefits from slightly less attenuated signal.

By considering the interference effect, SIR versus CFO for the transceivers with different spectral efficiencies are depicted in Fig. 4. Similar to the C, SIR is also an even function with respect to CFO. As expected, with lower spectral efficiency M/K, i.e. larger subband spacing, better immunity against CFO can be achieved. We can observe that SIR value dramatically increase when $\mu \to 0$, which is consistent with the results in Section IV-A. Moreover, the lowest SIR in the range of smaller CFOs (which is more common) are for the most spectral efficient FBMC system with $M = 64$ and $K = 72$. On the other hand, the highest SIR corresponds to two less efficient systems with $K = 112, 128$. One of them ($K = 128$) is benefiting from large subband spacing while the other one ($K = 112$) takes advantage of its long prototype filter and relatively large subband spacing. In the range of larger CFOs, $\mu > 20\%$, spectral efficiency η differentiates the curves placement. In this range of μ, better SIR ratios can be achieved by sacrificing the spectral efficiency.

B. Bit-error-rate

In order to practically asses the effectiveness of oversampling against CFO, the BER of FBMC systems in AWGN and frequency-selective channels are compared. Consider the channel model (3), in case of frequency-selective channel, it has been modelled to consist of $Q = 5$ independent Rayleigh-fading taps with an exponentially decaying power delay profile, i.e. $E[|c(l)|^2] = \alpha e^{-l/4}, l \in \{0, \cdots, Q-1\}$, where α is a constant such that $\sum_{l=0}^{Q-1} E[|c(l)|^2] = 1$. Since the number of subbands is relatively large $M = 64$ each subchannel could be approximated by a flat complex gain. Thus, employing

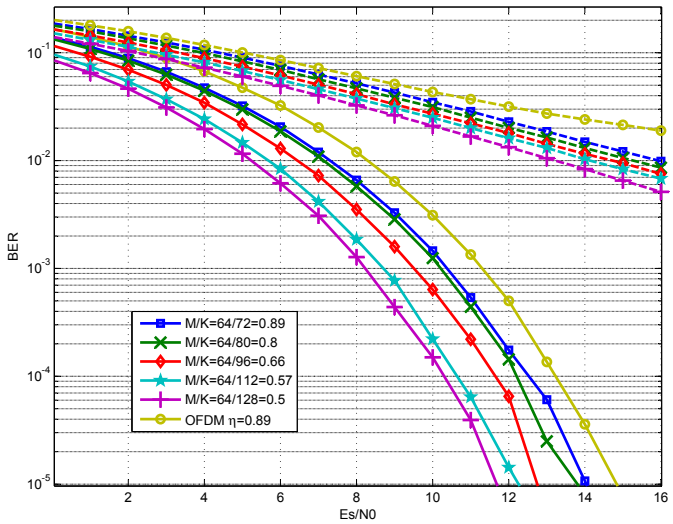

Fig. 5. BER vs. E_s/N_0 with CFO value $\mu = 5\%$ (solid lines: AWGN channel; dashed lines: frequency-selective channel).

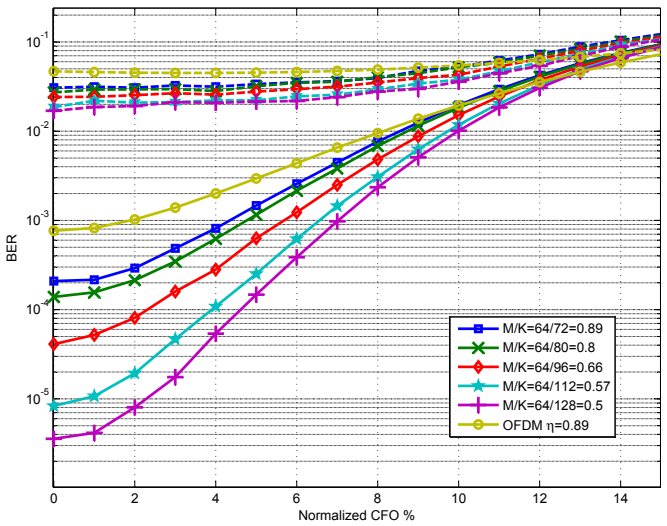

Fig. 6. BER vs. CFO with SNR $E_s/N_0 = 10$ dB (solid lines: AWGN channel; dashed lines: frequency-selective channel).

a simple one-tap per subband equalizer is sufficient to combat the frequency selectivity of the channel. Moreover, the channel is fixed in each run but independent from one run to another, where a number of 10^4 Monte Carlo trials has been performed. Note that, in case of AWGN channel, $Q = 1$ and $c[0] = 1$. For comparison purposes, the performance of OFDM system having $M = 64$ subcarriers with similar equalizer is also provided. Since CP can just remove ISI and larger CP length does not lead to reduction of CFO induced ICI [1], [9], we only report the ISI-free OFDM where the length of CP is longer than channel impulse response $L = 8$, where $\eta = \frac{M}{M+L} = 0.89$.

The BER of the mentioned FBMC systems and OFDM for different signal to noise ratios (SNR), i.e., E_s/N_0 and CFO values are depicted in Fig. 5 and Fig. 6, respectively. In Fig. 5, there is a fixed CFO $\mu = 5\%$ in all the transceiver systems. It is visible that OFDM has the worst BER among all the schemes. Moreover, to have a same BER in AWGN and frequency-selective scenarios among all the FBMC systems, by reducing 8% of spectral efficiency, 0.5 dB gain can be achieved.

In Fig. 6, we varied CFO value from 0 to 15% while keeping the SNR value $E_s/N_0 = 10$ dB fixed for all the schemes. It can be observed that BER increases monotonically as CFO increases. For the small CFOs ($\mu < 2\%$), the dominant interference factor is background noise. Therefore, the BER is not affected relatively for all the schemes in that range of CFO. However, as CFO increases, the CFO induced interferences become the dominant hindrance, which is confirming the results presented in Fig. 4. By sacrificing spectral efficiency, lower BER could be expected, as FBMC system with $\eta = 0.5$ can tolerate up to 7% more CFO compared to OFDM while having same BER. Furthermore, by decreasing the spectral efficiency of FBMC systems for roughly 8%, robustness against 1% more CFO can be achieved to have a same BER in both channels.

VI. Conclusion

The effect of different oversampling ratios for FBMC transceivers have been analyzed and compared in the presence of CFO. Generally, in addition to attenuating the signal, CFO can introduce various interference components including ISI and ICI. By analyzing the demodulated signal at the receiver, we were able to investigate the interference terms and derive SIR of the system. A better understanding of the tradeoff between the spectral efficiency and system performance is provided by obtained SIR. In addition to confirming the analysis, the experimental results exhibited the gained robustness against CFO by oversampling in FBMC systems.

References

[1] P. Moose, "A technique for orthogonal frequency division multiplexing frequency offset correction," *IEEE Trans. Commun.*, vol. 42, no. 10, pp. 2908–2914, Oct. 1994.

[2] T. Pollet, M. Van Bladel, and M. Moeneclaey, "BER sensitivity of OFDM systems to carrier frequency offset and Wiener phase noise," *IEEE Trans. Commun.*, vol. 43, pp. 191–193, Feb. 1995.

[3] P. Dharmawansa, N. Rajatheva, and H. Minn, "An exact error probability analysis of OFDM systems with frequency offset," *IEEE Trans. Commun.*, vol. 57, no. 1, pp. 26 –31, Jan. 2009.

[4] P. P. Vaidyanathan, *Multirate Systems and Filter Banks*. Upper Saddle River, NJ, USA: Prentice-Hall, 1993.

[5] G. Cherubini, E. Eleftheriou, and S. Olcer, "Filtered multitone modulation for very high-speed digital subscriber lines," *IEEE J. Sel. Areas Commun.*, vol. 20, no. 5, pp. 1016–1028, Jun. 2002.

[6] S. Rahimi and B. Champagne, "Perfect reconstruction DFT modulated oversampled filter bank transceivers," in *Proc. EUSIPCO*, Aug. 2011, pp. 1588–1592, Barcelona, Spain.

[7] B. Farhang-Boroujeny, "OFDM versus filter bank multicarrier," *IEEE Signal Process. Mag.*, vol. 28, no. 3, pp. 92–112, 2011.

[8] A. Assalini and A. Tonello, "Time-frequency synchronization in filtered multitone modulation based systems," in *Proc. WPMC*, Oct. 2003, pp. 221–225, Yokosuka, Japan.

[9] Q. Bai and J. Nossek, "On the effects of carrier frequency offset on cyclic prefix based OFDM and filter bank based multicarrier systems," in *Proc. SPAWC*, June 2010, pp. 1–5, Marrakech, Morocco.

[10] H. Saeedi-Sourck, Y. Wu, J. Bergmans, S. Sadri, and B. Farhang-Boroujeny, "Complexity and performance comparison of filter bank multicarrier and OFDM in uplink of multicarrier multiple access networks," *IEEE Trans. Signal Process*, vol. 59, no. 4, pp. 1907 –1912, April 2011.

[11] T. Wang, J. G. Proakis, and J. R. Zeidler, "Interference analysis of filtered multitone modulation over time-varying frequency- selective fading channels," *IEEE Trans. Commun.*, vol. 55, no. 4, pp. 717–727, 2007.

[12] T. Fusco, A. Petrella, and M. Tanda, "Sensitivity of multi-user filter-bank multicarrier systems to synchronization errors," in *Proc. ISCCSP*, March 2008, pp. 393–398, St. Julians, Malta.